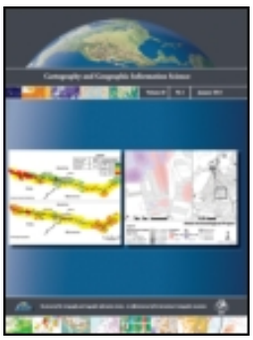

Taylor & Francis
Taylor & Francis Group

Cartography and Geographic Information Science

ISSN: 1523-0406 (Print) 1545-0465 (Online) Journal homepage: https://www.tandfonline.com/loi/tcag20

An Evaluation of Fractal Methods for Characterizing Image Complexity

Nina Siu-Ngan Lam , Hong-lie Qiu , Dale A. Quattrochi & Charles W. Emerson

To cite this article: Nina Siu-Ngan Lam , Hong-lie Qiu , Dale A. Quattrochi & Charles W. Emerson (2002) An Evaluation of Fractal Methods for Characterizing Image Complexity, Cartography and Geographic Information Science, 29:1, 25-35, DOI: 10.1559/152304002782064600

To link to this article: https://doi.org/10.1559/152304002782064600

An Evaluation of Fractal Methods for Characterizing Image Complexity

Nina Siu-Ngan Lam, Hong-lie Qiu, Dale A. Quattrochi and Charles W. Emerson

ABSTRACT: Previously, we developed an integrated software package called ICAMS (Image Characterization and Modeling System) to provide specialized spatial analytical functions for interpreting remote sensing data. This paper evaluates three fractal dimension measurement methods that have been implemented in ICAMS: isarithm, variogram, and a modified version of triangular prism. To provide insights into how the fractal methods compare with conventional spatial techniques in measuring landscape complexity, the performance of two spatial autocorrelation methods, Moran's I and Geary's C, is also evaluated. Results from analyzing 25 simulated surfaces having known fractal dimensions show that both the isarithm and triangular prism methods can accurately measure a range of fractal surfaces. The triangular prism method is most accurate at estimating the fractal dimension of surfaces having higher spatial complexity, but it is sensitive to contrast stretching. The variogram method is a comparatively poor estimator for all surfaces, particularly those with high fractal dimensions. As with the fractal techniques, spatial autocorrelation techniques have been found to be useful for measuring complex images, but not images with low dimensionality. Fractal measurement methods, as well as spatial autocorrelation techniques, can be applied directly to unclassified images and could serve as a tool for change detection and data mining.

KEYWORDS: Fractal measurement, spatial autocorrelation, simulated surfaces, data mining

Introduction

The rapid increase in digital data volumes from new sensors, such as NASA's Earth Observing System (EOS), Landsat-7, and commercial satellites, raises a critical problem—how can such an enormous amount of data be handled and analyzed efficiently? Efficient handling and analysis of large spatial data sets is central to research that utilizes various layers of information in different time periods. For example, long-term global change investigations require that new high-resolution data be combined with older, lower resolution images. Analyses of natural disasters such as hurricanes, fires, and earthquakes typically use time series of satellite imagery for rapid change detection and continuous monitoring. Advances in this type of large-scale spatial research require not only high-quality data sets, but also reliable tools to handle and analyze these data sets.

In a previous project, we developed a software module called ICAMS (Image Characterization and Modeling System) to address the above need by focusing on the development of innovative spatial analytical tools and then bundling the tools together in a module so that it can be accessed by the broader research community. Detailed descriptions of the theoretical background and the practical need for developing ICAMS, as well as its system design and functionality, can be found in Quattrochi, et al. (1997) and Lam, et al. (1998). In brief, ICAMS is a software module designed to run on Intergraph-MGE and Arc/Info platforms that provides specialized spatial analytical functions for characterizing remote-sensing images. The main functions of ICAMS are fractal analysis, variogram analysis, spatial autocorrelation analysis, texture analysis, land/water and vegetated/non-vegetated boundary delineation, temperature calculation, and scale analysis.

This paper focuses on the use of the fractal module in ICAMS. Specifically, we evaluate the performance of three fractal surface measurement algorithms that have been identified in the

Nina Lam is R. J. Russell Professor of Geography, Louisiana State University, Baton Rouge, LA 70803, USA. E-mail: <nlam@lsu.edu>. **Hong-lie Qiu** is assistant professor of Geography, California State University, Los Angeles, CA 90032, USA. E-mail: <hqiu@calstatela.edu>. **Dale Quattrochi** is Geographer/Senior Research Scientist at NASA Global Hydrology and Climate Center, Marshall Space Flight Center, AL 35812, USA. E-mail: <dale.quattrochi@msfc.nasa.gov>. **Charles Emerson** is Assistant Professor of geography, Western Michigan University, Kalamazoo, MI 49008, USA. E-mail: <charles.emerson@wmich.edu>.

literature and implemented in ICAMS: isarithm, variogram, and triangular prism. The purpose of this study is to provide benchmark information on the applicability and reliability of these fractal methods for characterizing landscape complexity using remote sensing imagery.

Fundamental research on the applicability and reliability of new spatial analytical techniques, such as fractals, is necessary. Although the fractal technique has been applied extensively, its use as a spatial technique for characterizing remote sensing images is rather uncommon and needs to be evaluated more thoroughly. In the past, it was difficult to apply the fractal technique because fractal algorithms were scattered throughout the literature of diverse disciplines such as meteorology (Lovejoy and Schertzer 1985), astronomy (Barbanis et al. 1999), and materials science (Lu and Hellawell 1995), and they were not necessarily designed to work with remote sensing images. With ICAMS and its fractal module, where the three major surface measurement methods identified in the literature (isarithm, variogram, and triangular prism) are modified and implemented, fractal measurement has become easier.

In this study, fractional Brownian motion (fBm) surfaces with known fractal dimensions are generated to evaluate the performance of the three fractal surface measurement methods. A comparison between known and computed fractal dimensions provides an assessment of the reliability and effectiveness of the three fractal methods for characterizing and measuring landscape patterns. Furthermore, to provide insight into how the fractal methods compare with conventional spatial techniques in measuring landscape complexity, this study also evaluates the performance of two spatial autocorrelation methods: Moran's I and Geary's C. Finally, since fractals are of particular use in determining the effects of changes in pixel resolution as a result of image processing, a sensitivity analysis of the response of the fractal and spatial autocorrelation indices is conducted.

An Overview of Fractals

Fractal techniques were developed because most spatial patterns of nature, such as curves and surfaces, are so irregular and fragmented that classical (Euclidean) geometry fails to provide tools for the analysis of their forms. In Euclidean geometry, a point has an integer topological dimension of zero, a line is one-dimensional, an area has two dimensions, and a volume three dimensions. In fractal geometry, the *fractal dimension* (D), is a non-integer value that, in Mandelbrot's (1983) original definition for fractals, exceeds the Euclidean topological dimension. As the form of a point pattern, a line, or an area feature grows more geometrically complex, the fractal dimension increases. The fractal dimension of a point pattern can be any value between zero and one, a curve between one and two, and a surface between two and three. Increasing the geometrical complexity of a perfectly flat two-dimensional surface (D=2.0) so that the surface begins to fill a volume, results in D values approaching 3.0.

Self-similarity is the foundation for fractal analysis (Mandelbrot 1983), and is defined as a property of a curve or surface where each part is indistinguishable from the whole, or where the form of the curve or surface is invariant with respect to scale. The degree of self-similarity, expressed as a self-similarity ratio, is used to define the theoretical fractal dimension. In practice, a common way to estimate the D value of a curve (e.g., a coastline) is to measure the length of the curve using various step sizes. The more irregular the curve, the greater the increase in length as step size increases. D can be estimated by the following equations:

$$Log\ L = K + B\ Log\ \delta \quad (1)$$

$$D = 1 - B \quad (2)$$

where:

L = length of the curve;
δ = step size;
B = slope of the regression; and
K = a constant.

From the above equations, D is a function of the regression slope B. The steeper the negative slope (B is a negative value), the higher the fractal dimension. The D value of a surface can be estimated in a similar fashion and is discussed in the next section.

Applications of fractals generally fall into two groups. The first uses the fractal model to simulate real-world objects for both analytical and display purposes. Fractals are commonly used in computer graphics because they can simulate life-like landscapes, cities, or objects for video games, movies, and a variety of virtual reality applications (Peitgen and Saupe 1988; Batty and Longley 1994). Moreover, simulated fractal surfaces (fractional Brownian motion (fBm) surfaces) or curves are regarded as ideal theoretical test data sets for testing a number of methods and models (Goodchild 1980; Goodchild and Mark 1987). In cartography and GIS, for example, fractal surfaces have been

used as test data sets to examine the performance of various spatial interpolation methods (Lam 1980) and the efficiency of a quadtree data structure (Mark and Lauzon 1984).

The second group of applications utilizes the fractal dimension as an index for describing the complexity of curves and surfaces. Goodchild (1980) demonstrated that fractal dimension could be used to predict the effects of cartographic generalization and spatial sampling, a result which may assist in determining the optimum resolution of pixels and polygons used in remote sensing and GIS studies. Various applications of fractals in geography and the geosciences, such as characterizing topography (Goodchild and Mark 1987) and urban landscapes (Batty and Longley 1994), have been documented in the literature. In particular, fractal analysis has been suggested as a useful technique for characterizing remote sensing images as well as identifying the effects of scale changes on the properties of images (De Cola 1989, 1993; Lam 1990; Lam and Quattrochi 1992; Emerson et al. 1999).

While the fractal model is a fascinating tool for simulation, its use as a technique for measuring and characterizing spatial phenomena has raised criticisms (Goodchild and Mark 1987; Lam 1990). At the theoretical level, the self-similarity property underlying the fractal model assumes that the form or pattern of the spatial phenomena remains unchanged throughout all scales, which further implies that one cannot infer the scale of the spatial phenomena from its form or pattern. This has been considered unacceptable in principle by a number of researchers. Empirical studies have shown that most spatial phenomena are not pure fractals with a constant D, but instead D varies across a range of scales. Rather than using D in the strict sense as defined by Mandelbrot (1983), many researchers nowadays realize that strict self-similarity is rare in natural phenomena, and that self-similarity must be estimated statistically and at certain scale ranges (Milne 1991). These findings, however, can be used positively. Lam and Quattrochi (1992) suggested that information on the changes of D with scale could be used to summarize the scale changes of the phenomena and to interpret their underlying processes at specific ranges.

At the technical level, a major impediment to applying fractal measurements is that there are very few algorithms readily available to researchers for experimentation. For those who can access the fractal algorithms, the frustration is that the results from applying differing algorithms often contradict each other (Tate 1998). A thorough evaluation of the various fractal measurement techniques, such as the three fractal techniques mentioned above, is necessary before they can be used to reliably characterize and compare changes in landscapes. Integrated software packages such as ICAMS make it easier to carry out the evaluation tasks.

In a broader sense, the fractal technique may be considered a textural measure for measuring image complexity. As with other texture-based analytical techniques such as co-occurrence matrices (Haralick et al. 1973), local variance (Woodcock and Strahler 1987), wavelets (Mallat 1989), and spatial autocorrelation statistics (Cliff and Ord 1973), fractals have shown great potential in characterizing landscape patterns for global environmental studies. Unlike many spatial indices used in landscape ecology such as contagion, dominance, and interspersion, the three fractal measurement methods and the spatial autocorrelation statistics implemented in ICAMS can be applied directly to unclassified images. This property makes them potentially useful tools for summarizing the spatial characteristics of the image (i.e., metadata representation), data mining, and change detection without the need for prior image classification. Ultimately, these methods can be used for environmental assessment and monitoring. A thorough evaluation and comparison of these methods is needed to identify their pros and cons in characterizing remote-sensing images.

Methods

Fractional Brownian Surfaces

To provide a benchmark for evaluating the three fractal surface measurement methods and the indices of spatial autocorrelation (Moran's I and Geary's C), fractional Brownian motion (fBm) surfaces with varying degrees of complexity (i.e., fractal dimension) were generated using the shear displacement method (Peitgen and Saupe 1988; Goodchild 1980; Lam and De Cola 1993; Tate 1998). The method starts with a surface of zero altitude represented by a matrix of square grids. A succession of random lines or cuts across the surface is then generated, and the surface is displaced vertically along each random line to form a cliff. This process is repeated until several cliffs are created between adjacent sample points. The set of random lines generated has the property that their points of intersection form a Poisson point process, while the angles of intersection are distributed

uniformly between 0 and 2π. The heights of the cliffs are controlled by the parameter H, which determines how the variance between two points relates to the separation distance. In other words, H describes the persistence of the surface and has values between 0 and 1. H is defined as:

$$E[z_i - z_{(d+i)}]^2 = |d|^{2H} \quad (3)$$

where $E[z_i - z_{(d+i)}]^2$ is the expected variance between two points having a distance d. The fractal dimensions of the simulated surfaces are equal to $D = 3 - H$ (Mandelbrot 1975; Goodchild 1980; Lam 1980).

Figure 1 shows the effect of the H parameter. A surface with $D = 2.1$ ($H = 0.9$) is quite smooth with similar z values occurring in adjacent areas. Increasing D to 2.5 results in a less smooth, less uniform surface. The surface with $D = 2.9$ ($H = 0.1$) is quite rough, with high and low values occurring at closely spaced intervals. The FORTRAN code for generating these fractal surfaces can be found in Lam and De Cola (1993).

To test which method (both fractals and spatial autocorrelation) measures image complexity more accurately, five 512 x 512 surfaces for each H level (0.1, 0.3, 0.5, 0.7, and 0.9) were generated using 3000 cuts. For each set of surfaces with varying H, identical seed values were used in order to generate the same sequence of random cuts and, therefore, visualize more easily the increase of complexity as H decreases. The resulting files were converted to 8-bit images normalized to digital numbers from 0 to 255. This generated five sets of simulated surfaces with fractal dimensions of 2.1, 2.3, 2.5, 2.7, and 2.9.

Fractal Measurement Methods

The three fractal surface measurement methods that have been implemented in ICAMS—the isarithm, variogram, and triangular prism methods—have been applied to real data and documented in detail in various studies (e.g., Lam and De Cola 1993; Jaggi et al. 1993; Xia and Clarke 1997). Except in a preliminary study (Lam et al. 1997), however, they have not been systematically evaluated using controlled, synthetic surfaces with a range of spatial complexity. The use of controlled surfaces provides a standard for comparison, thereby illuminating the major characteristics and differences among the methods.

The isarithm method uses the length of contours of surface z-values as a means of determining the fractal dimension D of the surface, where $D_{surface} = D_{isarithm} + 1$. The addition of "1" is needed to extend from a one-dimensional curve to a two-dimensional surface measurement. Analogous to the walking-divider method for measuring lines, the algorithm implemented in ICAMS evolved from methods proposed in Goodchild (1980), Shelberg et al. (1983), and Lam and De Cola (1993). In order to use the isarithm method in ICAMS, a data matrix of a given number of rows and columns must be specified, with the following parameter input by the user: the number of step sizes to be used to measure the length of the isarithm; the isarithm interval (to determine which isarithm is going to be measured); and the direction from which the operation proceeds (either row, column, or both).

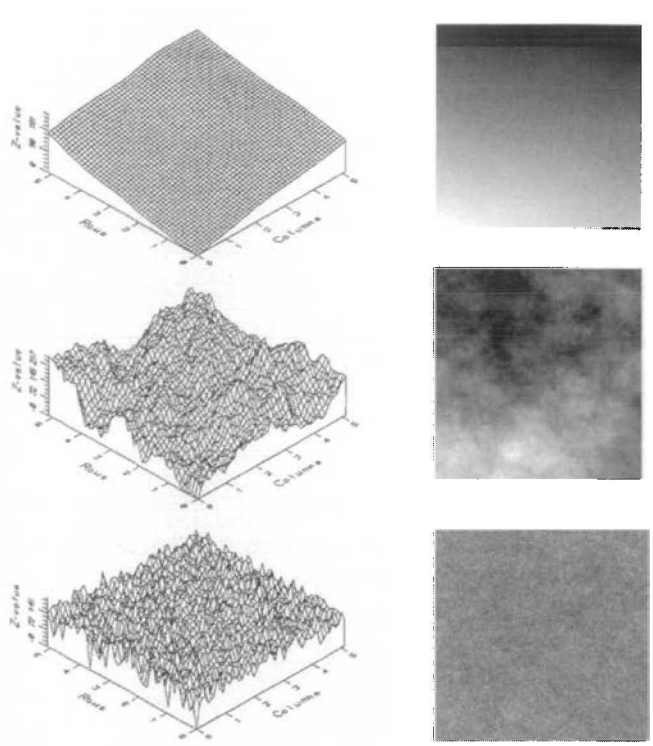

Figure 1. Three simulated surfaces and corresponding images from top to bottom, D = 2.1, 2.5, and 2.9.

For each isarithm value and step size, the algorithm classifies pixels below and above the isarithm value as white and black, respectively. It then compares each neighboring pixel along the rows or columns and determines if the pairs are both black or both white. If they are of different colors, it implies that an isarithm lies between two neighboring pixels, which are then recorded as boundary pixels. The length of each isarithm line is approximated by the total number of boundary pixels. It is possible that for a given step size there are no boundary pixels. In this case, the missing isarithm line is excluded from the analysis. The

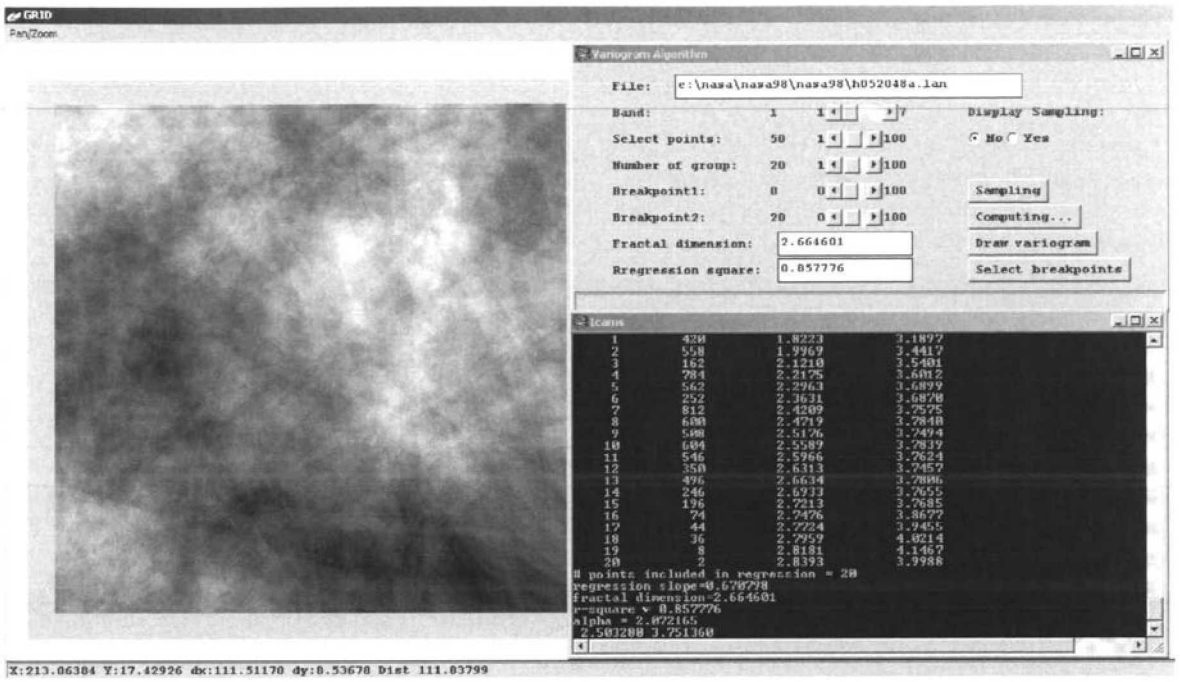

Figure 2. Sample output of a fractal analysis using the variogram method. The image on the left is a simulated fractional Brownian surface of 512x512 pixels with a theoretical D = 2.5. The screen on the right shows that the computed D is 2.66 with a regression fit $r^2 = 0.86$. The parameters used in the calculation were 20 distance groups and a sampling interval of every 50th point.

total number of boundary pixels for each step size is plotted against step size in log-log form (forming the fractal plot), and a linear regression is performed. The regression slope b is used to determine the fractal dimension of the isarithm line, where $D = 2\text{-}b$. The final D of the surface is the average of D values for those isarithms that have an R^2 greater than or equal to 0.9.

The variogram method uses the variogram function to estimate the fractal dimension. The variogram function describes how variance in surface height between data points relates to their spatial distance; and it is commonly used in many other applications such as kriging for characterizing the spatial structure of a surface. The only difference between the traditional variogram used in fractal estimation is that in the present approach, distance and variance are portrayed in double-log form. To derive the variogram function for a surface, variance for all data pairs that fall into a specified distance interval, $r(d)$, is calculated by:

$$\gamma(d) = (1/2n) \sum_{i=1}^{n} [z_i - z_{(d+i)}]^2 \qquad (4)$$

where:

n = total number of data pairs that fall in distance interval d, and

z = surface value.

The slope of the linear regression performed between these two variables (in double log form) is then used to determine the fractal dimension D, where $D = 3 - (b/2)$. Mark and Aronson (1984) pioneered the use of the variogram method for fractal measurement. Detailed discussion of the method can also be found in Lam and De Cola (1993) and Jaggi et al. (1993). In ICAMS, the variogram method requires the following input parameters: the number of distance groups for computing the variance, the sampling interval for determining the number of points used in the calculation, and the sampling method (regular or stratified random). Sampling only a subset of points for calculation is necessary, especially for large data sets such as remote sensing imagery, since the computational intensity increases dramatically with an increasing number of data points.

Figure 2 shows a typical output from the variogram method in ICAMS on the Arc/Info platform. The window on the left is a simulated fractional Brownian surface of 512 x 512 pixels with a theoretical $D = 2.5$. The screen on the right shows that the computed D is 2.66 with a regression fit $r^2 = 0.86$. The parameters used in the calculation were 20 distance groups and a sampling interval of every 50th point.

The triangular prism method (Clarke 1986; Jaggi et al. 1993) constructs triangles by connect-

ing the heights or z-values at the four corners of a grid cell to its center, with the center height being the average of the pixels at the four corners. These triangular "facets" of the prism are then summed to represent the surface area. In the second step, the algorithm increases the step size from one pixel to two pixels, thus forming 2 x 2 composites of four adjacent pixels. The corners of each 2 x 2 pixel composite are defined by the values of the four adjacent 2 x 2 pixels, and the center value is their average. The areas of the triangular prisms for all 2x2 composites are then calculated and summed. The algorithm continues until it reaches to the maximum step size specified by the user. The logarithm of the total of all the prism facet areas at each step is plotted against the logarithm of step size (number of pixels), and the fractal dimension is calculated by performing a linear regression on the surface areas and step sizes.

The triangular prism method implemented in ICAMS is different from the original algorithm discussed in Clarke (1986) and Jaggi et al. (1993). We show below that step size (δ) instead of step size squared (δ^2) should be used to regress with the prism areas to derive the correct fractal dimension. Consider the basic equations for defining the dimension of a fractal curve such as the Koch Curve (Mandelbrot 1967; Feder 1988):

$$N(\delta) = K\delta^{-D} \tag{5}$$

$$L(\delta) = N(\delta)\delta = K\delta^{1-D} \tag{6}$$

where:

δ = step size;
$N(\delta)$ = number of steps;
$L(\delta)$ = length of the curve; and
K = a constant.

To extend the curve definition to area, we can deduce the following expression of fractal dimension for an object whose area is A and step size δ:

$$A(\delta) = N(\delta)\delta^2 = K\delta^{2-D} \tag{7}$$

Rearranging the above equation into logarithmic form becomes:

$$Log\, A = K + (2\text{-}D)\, Log\delta \tag{8}$$

where:

$B = (2\text{-}D)$ is the slope of the regression;
K = a constant, and therefore:

$$D = 2 - B \tag{9}$$

Hence, the original algorithm was modified and implemented in ICAMS (Zhao 2001).

Unlike the isarithm method, the triangular prism method can be affected by the range of z values because the method compares area (unit squared) with grid cell length (unit). This is an important property that was not pointed out in previous literature. In order to make the fractal dimensions of various surfaces calculated from the triangular prism method comparable, normalization of the z values is necessary. To demonstrate this effect, a sensitivity analysis of the three fractal dimension measurement methods was performed, and the effects of contrast stretching on the resultant fractal dimensions are demonstrated below.

Spatial Autocorrelation Methods

ICAMS also contains modules for analyzing the spatial autocorrelation of images. Moran's I and Geary's C, two indices of spatial autocorrelation (Cliff and Ord 1973), have been commonly used to measure the spatial autocorrelation of polygons, but they have seldom been applied to measure images. Thus, their performance needs to be evaluated and compared with that of the fractal methods. Moran's I is calculated from the following formula:

$$I(d) = \frac{n\sum_i^n \sum_j^n w_{ij} z_i z_j}{W\sum_i^n z_i^2} \tag{10}$$

where:

w_{ij} = weight at distance d, so that
w_{ij} = 1 if point j is within distance d of point i, otherwise w_{ij} = 0;
z's = deviations (i.e., $z_i = x_i - x_{mean}$ for variable x); and
W = the sum of all the weights where $i \neq j$.

Moran's I varies from +1.0 for perfect positive autocorrelation (a clumped pattern) to −1.0 for perfect negative autocorrelation (a checkerboard pattern).

Geary's C contiguity ratio, another index of spatial autocorrelation that is similar to Moran's I, uses the formula:

$$C(d) = \frac{(n-1)\sum_i^n \sum_j^n w_{ij}(x_i - x_j)^2}{2W\sum_i^n z_i^2} \tag{11}$$

with the same terms listed above. Geary's C normally ranges from 0.0 to 3.0, with 0.0 indicating positive autocorrelation, 1.0 indicating no autocorrelation, and values greater than 1.0 indicating negative autocorrelation.

Surface Fractal Dimension	Isarithm D	Triangular Prism D	Variogram D	Mean	Standard Deviation	Moran's I	Geary's C
2.9	2.9989	2.9114	3.0518	132.0440	23.4960	0.1838	0.8172
2.7	2.8525	2.7233	2.9752	127.6700	28.6640	0.8390	0.1610
2.5	2.5192	2.3703	2.7007	123.3600	42.5840	0.9949	0.0051
2.3	2.1661	2.0718	2.1853	128.6760	53.0580	0.9999	0.0001
2.1	2.0424	2.0390	2.0140	129.6000	57.3720	1.0000	0.0000

Table 1. Summary statistics for the simulated surfaces.

Image Resampling and Contrast Stretching

Image resampling is used when images are rectified, in analyses of scale effects, or when older, low-resolution imagery is combined with newer high-resolution images. Bilinear resampling uses the four closest neighbors to perform a two-dimensional linear interpolation to obtain the output cell value (the output cell can be of any size or orientation). This averaging process reduces the dynamic range of the output brightness values, which is frequently overcome by contrast stretching. The effects of this resampling procedure on the performance of different fractal and spatial autocorrelation methods vary. To investigate these effects, a 1024 x 1024 pixel fractional Brownian surface having a known fractal dimension of 2.9 was generated. This produced a complex surface in which the brightness values change rapidly within a short distance. Bilinear resampling was used to reduce the resolution of the image, resulting in resampled images having 512 x 512, 256 x 256, 128 x 128, and 64 x 64 pixels. The pixel sizes ranged from one pixel width in the original surface, to resampled pixels that were two, four, eight, and sixteen pixels wide.

Results and Discussion

Table 1 lists the descriptive statistics for the 512 x 512 simulated surfaces, which show that as D increases, the standard deviation of the surface generally decreases. Standard deviation does not measure the spatial arrangement of the bright and dark pixels, just their relationship to the mean brightness value. In other words, standard deviation, which is a non-spatial measure of variation, bears no relationship with D, a spatial measure of variation. A moderate inverse relationship between fractal dimension and standard deviation has also been reported in previous studies where real remote-sensing images were measured (Lam et al. 1998). In that study, it was suggested that both spatial and non-spatial indices, such as fractal dimension and standard deviation, could be used together to form a broad impression of an image even without viewing it. Therefore, they should be considered as part of the metadata (i.e., key descriptors) for the image. For example, when an image has a high standard deviation but a relatively low fractal dimension (such as the D=2.1 surface in Figure 1), the surface would most likely exhibit a spatially homogeneous pattern with a detectable trend. On the contrary, if an image has a low standard deviation but a high fractal dimension (such as the D=2.9 surface), the surface is much more fragmented and spatially varying.

Fractal Measurement Methods

The isarithm, triangular prism, and variogram fractal measurement methods were used on each of the 25 simulated surfaces. For the isarithm method, the input parameters were number of step sizes = 5, isarithm interval = 10, and direction of operation = both row and column. The input parameters for the variogram method were 20 distance groups and sampling every 20th pixel from both rows and columns of a regular grid. The only input parameter required by the triangular prism method is number of step sizes; as with the isarithm method, it was fixed to five step sizes. The slope of the regression based on these five steps was used to compute fractal dimension in the isarithm and triangular prism methods.

Figure 3 shows the average fractal dimension D for each of the five sets of fractional Brownian surfaces. The triangular prism method is the best estimator for the rougher surfaces with fractal dimensions of 2.9 and 2.7, although it is less accurate at D = 2.5 and 2.3. For fractal dimensions around 2.5, the isarithm method is the most accurate. All the methods underestimate the fractal dimension for the D = 2.3 and 2.1 surfaces. Root mean squared errors (RMSE) for each set of surfaces by each fractal method were

computed by taking the square root of the average of the sum of squared differences between the estimated and the theoretical fractal dimensions. The results are shown in Table 2. Both the isarithm and the triangular prism methods yield similar RMSE (0.1068 and 0.1082), and they are generally lower than that of the variogram method. The triangular prism method has the worst RMSE for $D = 2.3$ surfaces, but best RMSE for $D = 2.7$ and 2.9 surfaces. The isarithm method is generally the best estimator for the three smoothest surfaces, while the variogram method is a comparatively poor estimator for all of the surfaces, particularly those with higher fractal dimensions.

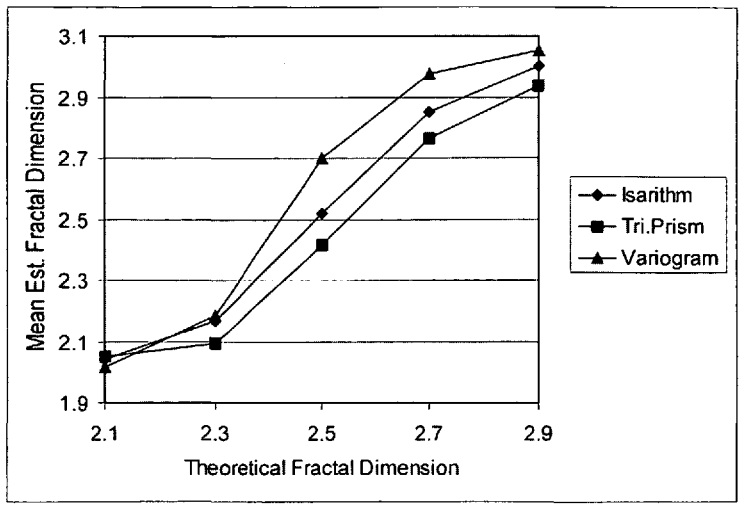

Figure 3. Comparison between mean estimated fractal dimension and theoretical fractal dimension.

Moran's I and Geary's C

As expected, there is an inverse relationship between Moran's I and Geary's C, as shown in Table 1 and displayed in Figure 4. The more complex surfaces with higher fractal dimension are more random in their spatial configurations and have Moran's I values close to 0.0 and Geary's C values close to 1.0 (negatively autocorrelated). The smoother surfaces with low fractal dimensions have Moran's I values of 1.0 and Geary's C values of 0.0 (positively autocorrelated).

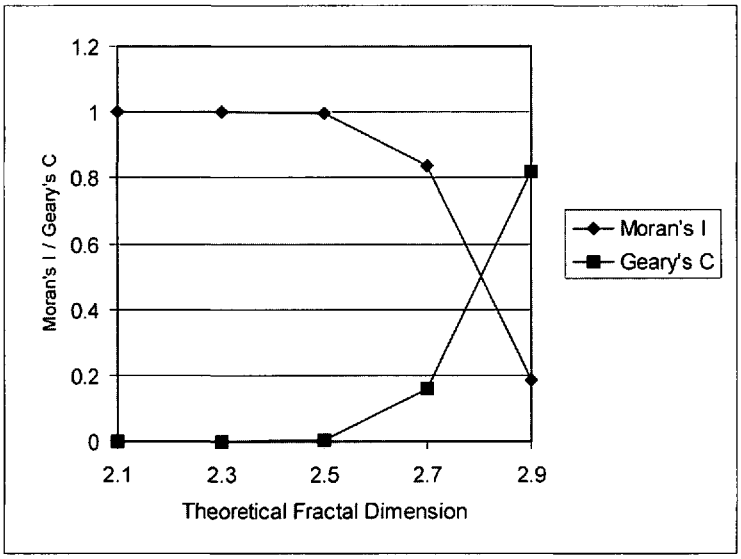

Figure 4. Relationship between theoretical fractal dimension and spatial autocorrelation indices.

Unlike the fractal methods, no RMSE were computed for the spatial autocorrelation statistics, as there were no theoretical spatial autocorrelation values for each set of D surfaces. However, the spatial autocorrelation values computed for each set of surfaces were very similar, with variance close to zero; therefore, the mean Moran's I and Geary's C values could be used to compare with the theoretical fractal dimension. In comparing the spatial autocorrelation statistics with the theoretical fractal statistics, the results presented in Figure 4 show that Moran's I (and by extension, Geary's C) could be used to measure the spatial complexity for surfaces with $D > 2.5$. Moran's I value decreases (Geary's C increases) as D increases, with a noticeble drop (jump for Geary's C) from $D = 2.7$ to $D = 2.9$. Although the range of Moran's I values is small, recent studies have shown that these small differences can be used to discriminate surface features as accurately as the fractal techniques (Myint 2001). For surfaces with lower fractal dimensions, this study shows that the spatial autocorrelation techniques are ineffective and do not reflect accurately the complexity of the simulated surfaces.

Resampling and Contrast Stretching

The triangular prism and isarithm methods for measuring fractal dimension and Moran's I and Geary's C indices of spatial autocorrelation were examined for their sensitivity to resampling and contrast stretching. The variogram method for measuring fractal dimensions was not evaluated in this analysis due to its instability when used on small images having relatively few pixels. A spatially complex, 1024 x 1024 fractional Brownian surface having a specified H value of 0.1 ($D = 2.9$) was used in this analysis. Figure 5 shows that

Surface Fractal Dimension	Isarithm	Triangular Prism	Variogram
2.9	0.1011	0.0463	0.1544
2.7	0.1532	0.0656	0.2818
2.5	0.0236	0.0845	0.3008
2.3	0.1364	0.2066	0.1575
2.1	0.0647	0.0478	0.0868
All Surfaces	0.1068	0.1082	0.2126

Table 2. Root mean squared error for estimated fractal dimension of the simulated surfaces.

the triangular prism method is strongly affected by reductions in image contrast. Smoothing an image by averaging larger and larger groups of pixels into a coarser resolution image results in a sharp drop off in D from slightly higher than the simulated value of 2.9 to a D value close to 2.5. Stretching the range of pixel values back to the original 0 to 255 range reduces the drop in measured fractal dimension.

The isarithm method is not as strongly affected by contrast stretching. In Figure 5, the isarithm method overestimates the simulated surface fractal dimension of 2.9, regardless of whether the dynamic range is restored by stretching or not. Since the isarithm interval is fixed, the fractal dimension is estimated from fewer isarithms in the unstretched images (when there is a smaller range of values) than it would be in an image stretched to the full dynamic range. For both the triangular prism and isarithm methods, the fractal dimension measurement is relatively stable as the image is resampled to coarser resolutions, as indicated by the generally horizontal trend in these plots (except in the case of unstretched triangular prism measurements). This is a characteristic of the ideal fractal nature of the fractional Brownian surfaces used in this analysis. The coarser versions of the original surface are similar in complexity to the original, particularly if they are normalized to the entire 0 to 255 dynamic range of pixel values. Real images of the earth depart from this fractal ideal, and often exhibit complex responses to changes in resolution (Emerson et al. 1999).

Figure 6 shows measurements of Moran's I and Geary's C on the same 1024 x 1024 images. In this case, contrast stretching has little effect on either index, although there is a tendency for the two indices to converge to a value of 0.5 as many smaller pixels are averaged into fewer larger ones.

Conclusions

The three fractal surface measurements methods implemented in ICAMS, including the isarithm, variogram, and modified triangular prism methods, were evaluated using 25 simulated surfaces of varying degrees of complexity. Based on the results from this analysis, we conclude that both the isarithm and triangular prism methods can be used to accurately analyze images over a range of fractal dimensions, although the triangular prism method is best for highly complex surfaces that are characteristic of remotely sensed imagery. The triangular prism method, however, is sensitive to the actual ranges of values. To ensure comparability and accuracy of measurement, the range of values should be normalized before computation by the triangular prism algorithm. The variogram method may not be appropriate for complex images, as it tends to yield higher fractal dimension estimates than the other methods. The variogram method, however, would be useful for measuring fractal surfaces of low dimensions. The spatial autocorrelation techniques are useful for measuring complex images, but not images with low dimensionality.

These results are useful for research on developing and improving spatial analytical techniques and our continuous updating and new implementations in ICAMS. These techniques could be used to examine a host of related research questions. For example, fractal measurement could be used to determine if different environmental and ecological landscapes and processes (e.g., coastlines, vegetation boundaries, and wetlands) have characteristic fractal dimensions. With accurate measurement methods, these fractal techniques could be used to identify regions of varying degrees of complexity, and ultimately be used as a part of metadata or as a tool for data mining or change detection without the need to classify images beforehand, thereby increasing the efficiency of continuous environmental monitoring. It is also possible to apply fractal techniques locally to achieve more accurate feature identification and change detection. Research is underway to explore these latest applications. For example, we are currently adding modules to ICAMS for local fractal and wavelet analysis. We also plan to further evaluate the applicability of these fractal and related spatial measurement methods for monitoring environmental changes in a number of localities, such as Xinjiang, China, and Atlanta, USA, where field investigations are currently underway. Furthermore, we will utilize the multi-resolution

property of different types of imagery and spatial data to gain a better understanding of the impact of scale on the analysis of environmental phenomena.

ACKNOWLEDGMENTS

This research was supported by a grant from NASA (Award number: NAGW-4221) and by NASA Summer Faculty Fellowships awards to Nina Lam and Charles Emerson. Additional support was also provided through a NASA Intelligent Systems research grant (NAS-2-37143). We thank Rajabushananum Cherukuri and Wei Zhao, then doctoral graduate assistants, for their technical assistance.

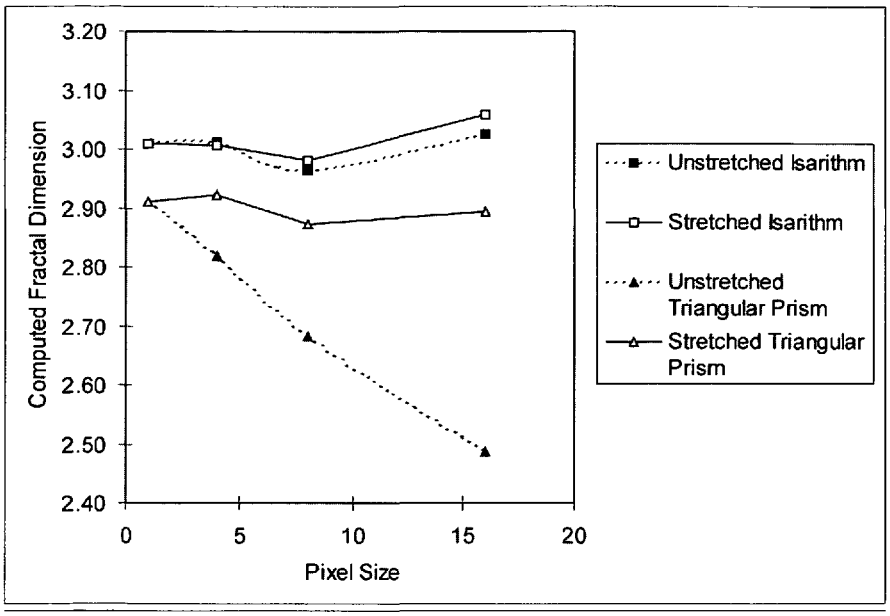

Figure 5. Effect of resampling and contrast stretching on computed fractal dimensions.

REFERENCES

Barbanis, B., H. Varvoglis, and C. L. Vozikis. 1999. Imperfect fractal repellers and irregular families of periodic orbits in a 3-D model potential. *Astronomy and Astrophysics* 344: 879-90.

Batty, M., and P. Longley. 1994. *Fractal cities: A geometry of form and function.* London, U.K.: Academic Press. 394 p.

Clarke, K. C. 1986. Computation of the fractal dimension of topographic surfaces using the triangular prism surface area method. *Computers & Geosciences* 12(5): 713-22.

Cliff, A. D., and J. K. Ord. 1973. *Spatial autocorrelation.* London, U.K.: Pion Limited. 178 p.

De Cola, L. 1989. Fractal analysis of a classified Landsat scene. *Photogrammetric Engineering and Remote Sensing* 55(5): 601-10.

De Cola, L. 1993. Multifractals in image processing and process imaging. In: N.S.-N. Lam and L. De Cola (eds), *Fractals in geography.* Englewood Cliffs, New Jersey: Prentice Hall. pp. 282-304.

Emerson, C. W., N. S.-N. Lam, and D. A. Quattrochi. 1999. Multi-scale fractal analysis of image texture and pattern. *Photogrammetric Engineering and Remote Sensing* 65(1): 51-61.

Feder, J. 1988. *Fractals.* New York, New York: Plenum Press.

Goodchild, M. F. 1980. Fractals and the accuracy of geographical measures. *Mathematical Geology* 12: 85-98.

Goodchild, M. F., and D. M. Mark. 1987. The fractal nature of geographic phenomena. *Annals of the Association of American Geographers* 77(2): 265-78.

Haralick, R. M., K. Shanmugam, and I. Dinstein. 1973. Textural features for image classification. *IEEE Transactions on Systems, Man, and Cybernetics* SMC-3: 610-21.

Jaggi, S., D. A. Quattrochi, and N. S.-N. Lam. 1993. Implementation and operation of three fractal measurement algorithms for analysis of remote-sensing data. *Computers & Geosciences* 19(6): 745-67.

Klinkenberg, B., and M. F. Goodchild. 1992. The fractal properties of topography: A comparison of methods. *Earth Surface Processes and Landforms* 17: 217-34.

Lam, N. S.-N. 1980. *Methods and problems of areal interpolation.* PhD Dissertation. London, Ontario: University of Western Ontario.

Lam, N. S.-N. 1990. Description and measurement of Landsat TM images using fractals. *Photogrammetric Engineering and Remote Sensing* 56(2): 187-95.

Lam, N. S.-N., and D.A. Quattrochi. 1992. On the issues of scale, resolution, and fractal analysis in the mapping sciences. *The Professional Geographer* 44(1): 89-99.

Lam, N. S.-N., and L. De Cola (eds). 1993. *Fractals in geography.* Englewood Cliffs, New Jersey: Prentice Hall. 308 p.

Lam, N. S.-N., H.-L. Qiu, and D. A. Quattrochi. 1997. An evaluation of fractal surface measurement methods using ICAMS (Image Characterization And Modeling System). *Technical Papers, ACSM/ASPRS Annual Convention, Vol. 5, Auto-Carto 13,* pp. 377-86. ACSM/ASPRS, Bethesda, Maryland.

Lam, N. S.-N., D. A. Quattrochi, H.-L Qiu, and W. Zhao. 1998. Environmental assessment and monitoring with image characterization and modeling system using multi-scale remote sensing data. *Applied Geography Studies* 2(2): 77-93.

Lovejoy, S., and D. Schertzer. 1985. Generalized scale invariance in the atmosphere and fractal models of rain. *Water Resources Research* 21: 1233.

Lu, S. Z., and A. Hellawell. 1995. Using fractal analysis to describe irregular microstructures. *Journal of Materials (JOM)* 47: 14-16.

Mallat, S. G. 1989. A theory for multi-resolution signal decomposition: The wavelet representation. *IEEE*

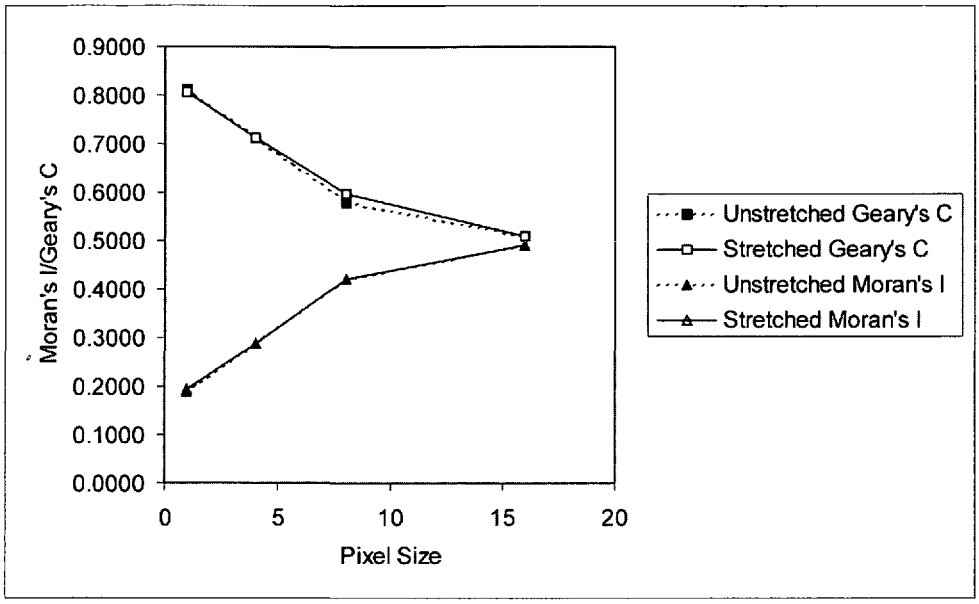

Figure 6. Effect of resampling and contrast stretching on Moran's *I* and Geary's *C*.

Transactions on Pattern Analysis and Machine Intelligence 11: 674-93.

Mandelbrot, B. B. 1975. On the geometry of homogeneous turbulence, with stress on the fractal dimension of the iso-surfaces of scalars. *Journal of Fluid Mechanics* 72: 401-16.

Mandelbrot, B. B. 1967. How long is the coast of Britain? Statistical self-similarity and fractional dimension. *Science* 155: 636-8.

Mandelbrot, B. B. 1983. *The fractal geometry of nature*. New York, New York: W. H. Freeman. 468 p.

Mark, D. M., and P. B. Aronson. 1984. Scale-dependent fractal dimensions of topographic surfaces: An empirical investigation, with applications in geomorphology and computer mapping. *Mathematical Geology* 11: 671-84.

Mark, D. M., and J. P. Lauzon. 1984. Linear quadtrees for geographic information systems. *Proceedings, International Symposium on Spatial Data Handling*, Zurich, Switzerland. pp. 412-430.

Milne, B.T. 1991. Lessons from applying fractal models to landscape patterns. In: M. G. Turner and R. H. Gardern (eds), *Quantitative methods in landscape ecology*. New York, New York: Springer Verlag. pp. 199-235.

Myint, S. W. 2001. *Wavelet analysis and classification of urban environment using high-resolution multispectral image data*. PhD Dissertation. Baton Rouge: Louisiana State University.

Peitgen, H.O., and D. Saupe (eds). 1988. *The science of fractal images*. New York, New York: Springer-Verlag.

Quattrochi, D. A., N. S.-N. Lam, H. L. Qiu, and W. Zhao. 1997. Image characterization and modeling system (ICAMS): A geographic information system for the characterization and modeling of multiscale remote-sensing data. In: D. A. Quattrochi and M. F. Goodchild (eds), *Scale in remote sensing and GIS*. Boca Raton, Florida: CRC/Lewis Publishers. pp. 295-307.

Shelberg, M. C., N. S.-N. Lam, and H. Moellering. 1983. Measuring the fractal dimensions of surfaces. In: *Proceedings, Sixth International Symposium on Automated Cartography (Auto-Carto 6)*, Ottawa, Canada, Vol. 2. pp. 319-28.

Tate, N. J. 1998. Estimating the fractal dimension of synthetic topographic surfaces. *Computers and Geosciences* 24(4): 325-34.

Woodcock, C. E., and A. H. Strahler. 1987. The factor of scale in remote sensing. *Remote Sensing of Environment* 21: 311-32.

Xia, Z.-G., and K. C. Clarke. 1997. Approaches to scaling of geo-spatial data. In: D. A. Quattrochi and M. F. Goodchild (eds), *Scale in remote sensing and GIS*, Boca Raton, Florida: Lewis Publishers. pp. 309-60.

Zhao, W. 2001. Multiscale analysis for characterization of remotely sensed images. PhD Dissertation. Baton Rouge: Louisiana State University.

XXII FIG International Congress
Washington 2002

ACSM/ASPRS Conference and Technology Exhibition 2002
Marriott Wardman Park Hotel,
Washington, D.C., USA.
April 19-26, 2002

ACSM Committee Meeting Schedule

Friday, April 19, 2002

2:00 pm – 6:00 pm	ACSM Strategic Planning Committee
2:00 pm – 6:00 pm	NSPS Restructure Committee

Saturday, April 20, 2002

8:00 am – 9:00 am	NSPS Board of Governors Orientation
8:00 am – 3:00 pm	ACSM Strategic Planning
8:00 am – 5:00 pm	ACSM Government Affairs Committee
8:00 am – 5:00 pm	ACSM/NSPS State Executives Forum
9:00 am – 11:00 am	NSPS Board of Governors Meeting
11:00 am – 1:00 pm	NSPS Standards Committee
11:00 am – 1:00 pm	NSPS Trig-Star Committee
11:00 am – 1:00 pm	NSPS Bylaws & Resolutions Committee
11:00 am – 2:00 pm	Great Lakes Regional Council
11:00 am – 2:00 pm	NSPS NAFTA Committee
11:00 am – 3:00 pm	NSPS Restructure Committee
11:00 am – 6:00 pm	NSPS County Surveyors Forum/ NACS Annual Meeting (Agenda can be found at www.acsm.net/nspsforum.html)
1:00 pm – 3:00 pm	Membership Development Committee
1:00 pm – 3:00 pm	NSPS/ALTA Committee
2:00 pm – 5:00 pm	NSPS Education Committee
3:00 pm – 5:00 pm	NSPS Professional Ethics & Liability Committee
3:00 pm – 6:00 pm	NSPS Private Practice Committee
5:00 pm – 6:00 pm	NSPS Youth Outreach Committee

Sunday, April 21, 2002

8:00 am – 10:00 am	ACSM Executive Committee
8:00 am- 10:00 am	NSPS Nominations Committee
8:00 am- 10:00 am	NSPS Public Relations Committee
8:00 am – 10:00 am	NSPS Mines & Minerals Committee
8:00 am – 12:00 pm	NSPS Editors Forum
8:00 am – 11:00 am	ACSM Education Committee
10:00 am – 11:00 am	NSPS Board of Governors Motions & Task Assignments
11:00 am – 1:00 pm	NSPS Board of Governors Task Force Meetings (Lunch)
1:00 pm – 4:00 pm	NSPS Board of Governors Meeting
1:00 pm – 5:00 pm	Hydrographer Certification Board
1:00 pm – 5:00 pm	Government Programs Committee
1:00 pm – 6:00 pm	ABET Training
2:00 pm – 5:00 pm	ACSM Communications Committee
2:00 pm – 5:00 pm	ACSM/US National Committee for ICA
3:00 pm – 5:00 pm	ACSM Elections Committee
3:00 pm – 5:00pm	ACSM Administrative Committee
4:00 pm – 5:00 pm	NSPS General Membership/Installation of Officers
5:00 pm – 7:00 pm	AAGS Board of Directors

Monday, April 22, 2002

7:00 am – 10:00 am	ACSM Fellows/NSPS Past President's Breakfast
8:00 am – 9:00 am	NSPS Policy Review Committee
8:00 am – 10:00 am	Surveyors Historical Society Board Meeting
9:00 am – 11:00 am	AAGS General Membership Meeting
9:00 am – 5:00 pm	NSPS Registration Board's Forum
10:00 am – 6:00 pm	NSPS Foundation, Inc. Board Meeting
10:00 am – 1:00 pm	Surveyors Historical Society Membership Meeting
10:00 am – 1:00 pm	ACSM CaGIS Editorial Board Meeting
1:00 pm – 2:00 pm	GLIS Board of Directors
1:00 pm – 5:00 pm	ACSM CAR Committee
2:00 pm – 4:00 pm	GLIS Membership Meeting
2:00 pm – 3:00 pm	ACSM Annual Conference Committee
3:00 pm – 5:00 pm	ACSM Admissions
4:00 pm – 6:00 pm	ACSM Workshop Committee
5:30 pm – 8:00 pm	ACSM Awards Ceremony

Tuesday, April 23, 2002

8:00 am – 5:00 pm	NSPS Board of Directors Meeting
8:00 am – 5:00 pm	CaGIS Board of Directors Meeting
10:00 am – 12:00 pm	ACSM Council of Sections
1:00 pm – 4:00 pm	ACSM Constitution & Bylaws Committee
1:00 pm – 2:00 pm	CaGIS Membership Meeting
4:00 pm – 6:00 pm	ACSM Spatial Data Standards

Wednesday, April 24, 2002

8:00 am – 5:00 pm	ACSM Board of Direction
9:00 am – 12:00 pm Exam	ACSM Hydrographer Certification
1:00 pm – 3:00 pm	NSPS Government Agency Forum